Lipid Desaturation Regulates the Balance between Self-renewal and Differentiation in Mouse Blastocyst-derived Stem Cells

Chanchal Thomas Mannully[1], Reut Bruck-Haimson[1], Anish Zacharia[1], Paul Orih[1], Alaa Shehadeh[1], Daniel Saidemberg[1], Natalya M Kogan[1], Sivan Alfandary[1], Raphael Serruya[1], Arie Dagan[1], Isabelle Petit[2]; Arieh Moussaieff[1]*

1. The Institute for Drug Research, The Hebrew University of Jerusalem, Jerusalem 9112102, Israel.
2. Sorbonne Université, Inserm, Centre de Recherche Saint-Antoine, CRSA, F-75012 Paris, France.

* To whom correspondence should be addressed at: ariehm@ekmd.huji.ac.il.

ABSTRACT

Stem cells are defined by their ability to self-renew and to differentiate, both shown in multiple studies to be regulated by metabolic processes. To decipher metabolic signatures of self-renewal in blastocyst-derived stem cells, we compared early differentiating embryonic stem cells (ESCs) and their extra-embryonic counterparts - trophoblast (T)SCs to their self-renewing counterparts. A metabolomics analysis pointed to the desaturation of fatty acyl chains as a metabolic signature of differentiating blastocyst-derived SCs via the upregulation of delta-6 desaturase (D6D; FADS2) and delta-5 desaturase (D5D; FADS1), key enzymes in the biosynthesis of polyunsaturated fatty acids (PUFAs). The inhibition of D6D or D5D by specific inhibitors or SiRNA retained stemness in ESCs and TSCs, and attenuated endoplasmic reticulum (ER) stress-related apoptosis. D6D inhibition upregulated stearoyl-CoA desaturase-1 (Scd1) in ESCs, essential to maintain ER homeostasis. In TSCs, however, D6D inhibition downregulated Scd1. TSCs show higher *Scd1* mRNA expression and high levels of monounsaturated fatty acyl chain products in comparison to ESCs. Addition of oleic acid – the product of Scd1 (essential for ESCs), to culture medium, was detrimental to TSCs. Interestingly, TSCs express a high molecular mass variant of Scd1 protein, hardly expressed by ESCs. Taken together, our data point to lipid desaturation as a metabolic regulator of the balance between differentiation and self-renewal of ESCs and TSCs. They point to lipid polydesaturation as a driver of differentiation in both cell types. In contrast, mono unsaturated fatty acids (MUFAs), known to be essential for ESCs is detrimental to TSCs.

KEYWORDS

Embryonic stem cells; Pluripotent stem cells; Trophoblast stem cells; Metabolomics; Lipid desaturation; D6D; FADS2; D5D; FADS1; Scd1; Apoptosis; Proliferation; ER stress; Self-renewal; MUFAs; PUFAs

INTRODUCTION

The regulation of cell viability by metabolic perturbations has been well-documented for a century. The set of small molecules ("metabolome") has accordingly emerged as an important means for a detailed examination of cell state. While most studies describing the metabolic regulation of cell state and cell viability, have been carried out on cancer cell lines, recent studies strongly suggest that metabolic perturbations also play major roles in stem cell (SC) biology.

The balance between self-renewal and differentiation of SCs of the blastocyst is critical for their function *in vitro* and *in vivo*, and enables the concerted development of the embryo. The blastocyst comprises an inner cell mass (ICM; consisting of the pluripotent epiblast, which generates the future embryo, and the extra-embryonic primitive endoderm), and the trophectoderm (1). During morula compaction and the formation of the blastocyst, cells undergo the first differentiation into ICM and trophoblast (2). Cells that are isolated from the ICM can be cultivated as embryonic (E)SCs, defined by their ability to differentiate into all adult cell types (3), hence pluripotent (P)SCs. Cells isolated from the trophectoderm give rise to the placenta (4, 5), and can be cultivated as trophoblast (T)SCs. Importantly, the low accessibility of early embryos, the paucity of embryonic material, and the technical difficulties in direct experimental manipulation *in vivo*, underscore the necessity of cell models for the study of early development (6). This is especially true for metabolic analyses, as there is no amplification of signal in such analyses, thereby requiring a relatively large amount of cells per sample.

Research during the last decade by several groups, including ours, has uncovered metabolic signatures of SC potency state (7-12), and roles played by metabolic shifts in the molecular circuitry that maintains stemness (7, 10, 11, 13-34). Metabolic perturbations also regulate self-renewal in pluripotent and adult SCs (13, 31, 35-39). Taken together, these studies suggest that the metabolic status of SCs is critical for the balance between self-renewal and differentiation in SCs.

We previously demonstrated a shift in glycolytic flux in PSCs upon their exit from pluripotency, driving differentiation via modification of histone acetylation (7). While shifts in central metabolism (7, 14, 19, 20, 24) and amino acid metabolism (11, 27) have been suggested to regulate the turnover and differentiation of SCs, information on the roles of

75 lipid pathways in SC biology is still lacking. Nevertheless, lipids represent a major energy
76 source during early development (40), and their content was reported to regulate the self-
77 renewal of human ESCs (41). In particular, phospholipids are involved in PSC
78 differentiation, as CDP-ethanolamine pathway synthesis of phosphatidylethanolamine is
79 required at the early stage of reprogramming to PSCs (42).

80 In a seminal study that provided an unbiased view of ESC metabolism vs
81 differentiated cells, Yanes and colleagues found highly unsaturated metabolite structures
82 in undifferentiated ESCs (9). Importantly, however, inhibition of polyunsaturated fatty acid
83 (PUFA) synthesis promoted pluripotency, suggesting that lipid polydesaturation may have
84 a unique non-redox role in the differentiation of ESCs. In mammalian cells, the rate limiting
85 enzyme in the conversion of saturated fatty acids (SFAs) to monounsaturated fatty acids
86 (MUFAs) is stearoyl-CoA desaturase (SCD). The two human isoforms of SCD are SCD1
87 and SCD5. SCD1 is the ubiquitous human orthologue of the mouse Scd1, whereas SCD5
88 is expressed in the brain and pancreas. Further support to the notion that the desaturation
89 of fatty acyl chains plays critical roles in SC metabolism was given by Ben-David and
90 colleagues, who demonstrated that SCD-1, also called Δ-9-desaturase, is essential for
91 ESC survival (37).

92 Here, we sought to reveal the metabolic events that take place upon early
93 differentiation of blastocyst-derived SCs, and in particular, the ICM-derived ESCs and
94 their extra-embryonic equivalents, the trophectoderm-derived TSCs, by comparing the
95 metabolic signatures of early differentiating SCs to their undifferentiated counterparts. We
96 found higher abundance of polyunsaturated acyl chains in both cell types upon early
97 differentiation. The inhibition of Δ6 desaturase (D6D, or FADS2) or Δ5 desaturase (D5D,
98 or FADS1) attenuated differentiation in both cell types, resulting in increased self-renewal.
99 Interestingly, Scd1 inhibition showed opposite effects on cell viability in ESCs and TSCs,
100 revealing distinct metabolic requirements between these two embryonic SC populations.
101

102 **RESULTS**

103 Our previous work demonstrated a metabolic shift in ESCs upon the exclusion of
104 growth factors that retain pluripotency, causing early differentiation (7). Following the
105 same approach, we now sought to unveil common and distinct metabolic regulatory

106 mechanisms of the balance between differentiation and self-renewal in ESCs and TSCs.
107 For this aim, we allowed ESCs or TSCs to differentiate, and compared their metabolic
108 profiles to these of their self-renewing counterparts.

109 ESCs were cultivated in feeder free conditions for at least 3 passages. 24 hours
110 after seeding, we initiated spontaneous differentiation, by exclusion of LIF and 2i from
111 feeder free culture medium, and collected cells for a metabolomics analysis 48 hours after
112 medium change. The medium of ESCs of the same experimental lot was replaced with
113 fresh ESC culture medium that contained LIF and 2i, and they were used as
114 undifferentiated control. We then compared the early differentiating ESCs to their
115 undifferentiated counterparts. The colonies of early differentiating ESCs showed a non-
116 condensed morphology with unclear borderlines (**Figure 1A**), suggesting their exit from
117 pluripotency. This observation was corroborated by decreased expression of the
118 pluripotency markers *Nanog* and *Sox2* (**Figure 1B**). No significant change was noted in
119 the expression of *Oct4*, known to be downregulated more slowly upon differentiation (43).
120 Partial least squares regression discriminant analyses (PLS-DAs) of the LC-MS-derived
121 metabolic profiles of the early differentiating vs the undifferentiated ESCs, was performed
122 following quantile normalization, and showed discrete metabolome of the early
123 differentiating ESCs (**Figure 1C**; R^2=0.89, Q^2=0.69 for blastocyst derived ESCs; R^2=0.93,
124 Q^2=0.84 for TNGA *Nanog* ESCs).

125 We cultivated TSCs in feeder free medium (See Materials and methods) for 3
126 passages, and then excluded FGF4, TGFβ and heparin from cultivation medium, to
127 initiate spontaneous differentiation. The medium of TSCs of the same experimental lot
128 was replaced with fresh TSC culture medium that contained FGF4, TGFβ and heparin,
129 and they were used as undifferentiated control. Early differentiation was confirmed by
130 morphology (**Figure 1D**) and the expression of TSC marker genes. Specifically, the TSC
131 marker gene *Elf5* was downregulated and the trophoblast lineage marker *Tfap2c* was
132 upregulated (**Figure 1E**) (44). The expression of *Eomes* and *Cdx2*, two more TSC
133 markers, did not significantly change. We compared the metabolome of TSCs after 48
134 hours of differentiation to that of their undifferentiated counterparts, and found a full
135 separation: *Oct4*-GFP M2rtTA homo BL6 TSCs (blastocyst derived TSC1; “BD TSC 1”;

136 R^2=0.99, Q^2=0.98), and *Oct4*-GFP M2rtTA hetero agouti ("BD TSC 2"; R^2=0.99, Q^2=0.91)
137 (**Figure 1F**).
138 After demonstrating the metabolic shift in ESCs and TSCs in standard cultivation
139 media, we wished to study these shifts in ESCs and TSCs, maintained in similar defined
140 cultivation medium. As TSCs have strict requirements for medium composition, and
141 cannot be maintained in conditions suitable for ESCs, we maintained ESCs and TSCs in
142 Tx basic medium, suitable for TSC cultivation (See Materials and Methods). We
143 supplemented Tx medium with FGF4, TGFβ and heparin for TSCs, or with LIF and 2i for
144 cultivation of ESCs. 24 hours following seeding, we allowed SCs to differentiate by
145 excluding the above factors from cultivation medium for 48 hours. The medium of SCs of
146 the same experimental lot was replaced with fresh ESC/TSC culture medium as above,
147 and they were used as undifferentiated control. We then compared the metabolic
148 composition of early differentiating SCs to that of undifferentiated cells. A PLS-DA
149 demonstrated a distinct common metabolic shift along the second principal component
150 (PC2), separating self-renewing SCs from early differentiating SCs (**Figure 2A**). To reveal
151 the metabolites responsible for the separation, we performed a variable importance in
152 projection (VIP) analysis. Of the 132 VIP>1 list of metabolic features, we noted a large
153 number of phospholipids (39). Of these, MS/MS experiments confirmed the putative
154 identifications of 19 phospholipids with more than two double bonds (polyunsaturated) in
155 their acyl chains. Notably, phospholipids with polyunsaturated acyl chains showed higher
156 abundances in early-differentiated TSCs and ESCs (**Figure 2B; Table S1**). The acyl
157 chain composition of phospholipids is an accurate and sensitive measure of fatty acid
158 incorporation into the cells (45). Accordingly, we assumed that the total content of
159 polyunsaturated lipid species in the early differentiating SCs is increased. In agreement
160 with this premise, we measured higher concentrations of total arachidonic acid in the early
161 differentiating ESCs (**Figure 2C-D**). We next wished to determine the enzymes
162 responsible for the shift in lipid desaturation in the early differentiating SCs.
163 Polydesaturation in animals requires sources for lipids with two double bonds, primarily
164 linoleic and α-linolenic essential fatty acids. Delta 6 desaturase (D6D; fatty acid
165 desaturase 2; FADS2) and delta 5 desaturase (D5D; FADS1) catalyze the synthesis of
166 PUFAs (**Figure 2E**). Aligned with the increased abundance of PUFAs, the expression of

167 *D6D* and *D5D* was upregulated upon early differentiation of ESCs (**Figure 2F**) and TSCs
168 (**Figure 2G**).
169 To examine the expression of markers of stemness in differentiation-inducing
170 culture conditions, we used SC-26196, a specific inhibitor of D6D. D6D inhibition retained
171 the expression of pluripotency marker genes in early differentiating ESCs (**Figure 2H)**,
172 and TSC marker genes in differentiating TSCs (**Figure 2I)**.
173 Taken together, these results suggest that differentiated ESCs and TSCs share
174 increased levels of polyunsaturated lipids. This shift can be attributed to D6D and D5D
175 expression, and is allocated at the exit from a self-renewing state.
176 We wished to better define the influence of polydesaturation on blastocyst derived
177 SCs. For this, we inhibited D6D or D5D in ESCs or TSCs of the same (129 / black 6)
178 background (main Figures), and validated the data from these experiments using
179 independent ESC and TSC lines (Supplemental Figures).
180 Microscopic examination of the cells suggested a higher number of colonies and
181 greater colony size in D6D inhibited ESCs. Indeed, D6D or D5D inhibition caused an
182 increase in ESC numbers (**Figure 3A-B)**, concomitant to an increase in clonogenicity
183 (**Figure 3C-D).** D6D inhibition in ESCs in a defined Tx medium also resulted in increased
184 proliferation of ESCs (**Figure 3E).** The effect of D6D inhibition on self-renewal was dose-
185 dependent (**Figure 3F)**, and specific, as confirmed by the inhibition of D6D by SiRNA
186 (**Figure 3G**).
187 The ability of cells to respond to perturbations in endoplasmic reticulum (ER)
188 function is critical for cell survival (46). Alterations in ER lipid composition result in ER
189 stress (47). In particular, ER function is associated with the degree of desaturation of
190 cellular fatty acyl chains (48, 49). We assumed that polydesaturation may decrease the
191 viability of ESCs by driving ER stress-related apoptosis. In line with this possibility, we
192 found reduced expression of the ER stress activators inositol-requiring transmembrane
193 kinase/endoribonuclease 1α (*IRE1*α) and activating transcription factor 6 (*ATF6*) upon
194 D6D inhibition (**Figure 3H**). D6D inhibition reduced the percentage of dead (**Figure 3I**)
195 and increased the percentage of pre-apoptotic and necrotic (**Figure 3J-K**) ESCs,
196 confirming an anti-apoptotic effect. To further confirm the pro-apoptotic influence of D6D
197 in ESCs, we tested its effect on the viability of further ESC lines (**Figure S1**). We also

198 wished to define the effect of D6D inhibition on ESC cell cycle, and found no effect (**Figure**
199 **S1**), suggesting that the higher proliferation rate is not due to cell cycle rate, and may be
200 attributed to less ER stress-related apoptosis, leading to higher viability of ESCs following
201 downregulation of D6D.

202 Similarly to ESCs, the inhibition of polydesaturation by D6D or D5D increased TSC
203 proliferation (**Figure 4A**), and the number of colonies (**Figure 4B**), concomitantly with
204 decreased expression of IRE1α (**Figure 4C**), and attenuation of apoptosis (**Figure 4D-**
205 **E**). Unlike in ESCs, the inhibition of D6D also increased the percentage of TSCs in S
206 phase (**Figure 4F-G**), suggesting that the increase in proliferation rate in TSCs is also
207 partially mediated by altered cell cycle kinetics. We validated the increased proliferation
208 of TSCs using independent TSC lines (**Figure S2**).

209 The cultivation of ESCs and TSCs is mostly done on feeder cells that release
210 factors that support SC cultivation. To evaluate the influence of D6D on SC proliferation
211 in feeder cell-based culture, we carried out FACS analyses of the ratio of SCs / mouse
212 embryonic fibroblasts (MEFs) in culture. We used *Oct4*-GFP labeled ESCs for the
213 quantification of ESCs. For the quantification of TSC proliferation in co-culture, we labeled
214 TSCs using an anti-CD40 (a TSC marker) antibody. ESC relative proliferation in culture
215 with feeder cells increased following the inhibition of D6D, whereas the number of D6D
216 inhibited TSCs only slightly and insignificantly increased in culture with the MEF feeder
217 cells (**Figure S3**).

218 A balance between mono- and poly-desaturation of lipids is maintained in the liver,
219 brain, lymphocytes and adipocytes, as PUFAs represses Scd1 activity and mRNA stability
220 (50-52). Scd1 inhibition activates the IRE1/XBP1s signaling arm of the unfolded protein
221 response, causing ER stress (53, 54). Interestingly, the stress response following Scd1
222 inhibition causes massive apoptosis in human ESCs, but not somatic cells; mouse ESCs
223 showed partial elimination (37). Accordingly, we reasoned that the increase in cell viability
224 in D6D inhibited ESCs may result from upregulation of Scd1 activity, leading to lower
225 apoptosis rates. In line with this hypothesis, *Scd1* was upregulated in ESCs following
226 inhibition of D6D (**Figure 5A**). Surprisingly, in contrast to the inverse regulation of *Scd1*
227 by D6D in ESCs, *Scd1* was downregulated upon D6D inhibition and downregulation in
228 TSCs, suggesting a reciprocal regulation of Scd1 in the two cell types by PUFAs (**Figure**

229 **5B**). Scd1 mRNA expression was slightly downregulated in early differentiating ESCs,
230 whereas a non-significant upregulation noted in TSCs (**Figure 5C**). We wished to further
231 examine possible functional implications of Scd1 expression in blastocyst-derived SCs.
232 The expression of the pluripotent markers *Oct4* and *Sox2* was downregulated in early
233 differentiating ESCs (**Figure 5D**), whereas TSC markers were upregulated in early
234 differentiating TSCs (**Figure 5E**) following inhibition of Scd1. The inhibition of Scd1 by
235 PluriSIn 1 was reported by Ben-David and colleagues to partially eliminate mouse ESCs
236 (37). Aligned with the results of this study, we saw partial elimination of mouse ESCs by
237 PluriSIn 1 or A-939572 - another Scd1 specific inhibitor (**Figure 5F-G**). Remarkably, the
238 inhibition of Scd1 in TSCs increased their viability (**Figure 5H-I**). The addition of
239 conjugated oleate to Scd1-inhibited TSCs attenuated their proliferation, reducing it to the
240 level seen in control cells (**Figure 5J**). As expected from the higher viability of TSCs upon
241 Scd1 inhibition, they showed decrease in the expression of ER stress genes **(Figure 5K)**,
242 and reduced apoptosis **(Figure 5L-M)**. We tested the viability of ESCs and SCs under
243 Scd1 inhabitation and confirmed that the increase in viability of TSCs, whereas decrease
244 of ESC viability by Scd1 inhibition is not cell line specific (**Figure S4**). Inhibition of Scd1
245 in feeder cell-based culture resulted in increased proliferation in TSCs, whereas lower
246 ESC proliferation (**Figure S5**).

247 We assumed that the detrimental influence of Scd1 on ESCs may reflect a
248 differential expression of the enzyme and its products. We found approximately one order
249 of magnitude higher gene expression of *Scd1* in TSCs (**Figure 5N**), and a corresponding
250 accumulation of MUFAs (**Figure 5O**). The examination of Scd1 protein expression
251 suggested a surprising alteration in the molecular weight of Scd1 in ESCs (molecular
252 mass ~35 kDa) and TSCs (molecular mass ~70 kDa) (**Figure 5P; Figure S6**). Upon early
253 differentiation, Scd1 protein expression is decreased in ESCs, with no change noted in
254 early differentiating TSCs (**Figure 5P; Figure S6**). MEFs (differentiated embryonic cells),
255 show no preference to either of the Scd1 variants (**Figure 5P; Figure S6**). Scd1 is
256 regulated by the availability of fatty acids (50). To better understand the shift in Scd1
257 variants and address a possible regulation of their expression by the availability of
258 external fatty acids, we incubated ESCs in 0-10% FBS (the source of external fatty acids).
259 Although we noted an upregulation of Scd1 with increasing percentage of serum, no

260 change in the high molecular mass variant of Scd1 was noted (**Figure S6**). Nevertheless,
261 we then examined the expression of Scd1 in ESCs and TSCs, cultivated in the same
262 defined (Tx) medium, and saw the same alteration in the Scd1 variant (**Figure 5Q**).
263 Notably, oleic acid – the product of Scd1, blocked the Scd1-dependent increase in viability
264 in D6D inhibited TSCs (**Figure 5R**), suggesting that this increase is mediated by the
265 downregulation of the basal high MUFA levels in TSCs.
266

267 **DISCUSSION**

268 In the current study, we characterized the metabolic profiles of early differentiating
269 ESCs and extra-embryonic TSCs vis-à-vis their self-renewing counterparts. Our
270 metabolomics analyses clearly show a metabolic shift in both blastocyst-derived SCs as
271 they exit self-renewal. This shift results in higher levels of PUFAs, following increased
272 expression of D6D and D5D. No change was seen in the levels of linoleic acid. The
273 inhibition of lipid polydesaturation by D6D or D5D retains self-renewal in ESCs and TSCs,
274 suggesting that PUFA levels are driving differentiation in both cell types, and that
275 controlling lipid desaturation is essential for the balance between self-renewal and
276 differentiation, and for the maintenance of ESCs and TSCs in culture.

277 Previous work suggests that the global metabolome of ESCs is characterized by
278 abundant metabolites with highly unsaturated structures, of which the levels decrease
279 upon differentiation (9), whereas the results of our analyses demonstrate upregulation of
280 lipid desaturation upon differentiation. This seeming discrepancy may be a result of our
281 focus on desaturation of lipids. It may also be attributed to variations in the differentiation
282 stage studied (early differentiated vs fully differentiated neurons or cardiomyocytes).
283 Despite this seeming discrepancy, our data on the retention of pluripotency by the
284 inhibition of lipid polydesaturation in ESCs are well aligned with the results of Yanes and
285 colleagues on ESC differentiation (9). Our results further link the shift in lipid
286 polydesaturation to lower SC self-renewal by exerting ER stress-related apoptosis.

287 The regulation of the ER status by lipid desaturation has been reported in multiple
288 studies in somatic cells. In ESCs, downregulation of Scd1 causes ER stress and
289 apoptosis, as demonstrated by Ben-David and colleagues (37), and by our results. Given
290 the regulation of Scd1 by PUFAs in the liver, lymphocyte, brain, and adipocytes cells (50),

291 we reasoned that lipid polydesaturation inversely regulates Scd1 in ESCs. Our results are
292 in concurrence with this assumption, suggesting that polydesaturation – a metabolic
293 signature of stemness, may modulate the ER status via regulation of Scd1 expression.
294 Surprisingly, we saw a downregulation of Scd1 following D6D inhibition in TSCs.
295 Despite the reciprocal regulation of Scd1 by D6D in ESCs vs TSCs, inhibition of
296 polydesaturation decreases ER stress and apoptosis in both cell types. The fact that Scd1
297 inhibition increases ESC death while increasing the viability of TSCs provides an
298 explanation for this, and underscores a unique essentiality of MUFAs in ESCs when
299 compared to their extra-embryonic counterparts.
300 The finding that TSCs express higher mRNA levels and a different protein variant
301 of Scd1, provides mechanistic insights into the differences in its essentiality and function.
302 A high molecular Scd1 variant, such as the one expressed In TSCs, was previously
303 attributed to the formation of dimers (55, 56). It was suggested to have potentially altered
304 function or stability (57), but it has not been isolated, and its function has so far not been
305 studied .
306 Our results show that while ESCs are addicted to MUFAs, TSCs have high levels
307 of MUFAs, high mRNA expression of Scd1, and an altered variant of Scd1 protein. The
308 addition of conjugated oleate to D6D-inhibited TSCs rescues apoptosis, supporting the
309 notion that increasing MUFA levels may be detrimental for TSCs, and linking the pro-
310 apoptotic effect of D6D to the regulation of MUFA levels.
311 Further research is required to establish the function of Scd1 variants and their
312 regulation by PUFAs in the early embryo. Seeing that the high molecular variant of Scd1
313 is expressed in the extraembryonic TSCs, it would be interesting to study its expression
314 and function in the placenta.
315 The downregulation of the expression of pluripotency markers by Scd1 inhibition
316 in ESCs may be a nonspecific toxic effect. Still, the upregulation of TSC marker genes by
317 Scd1 inhibition suggests that the regulation of the blastocyst-derived SC populations by
318 Scd1 is also mediated by modulation of the potency of the cells to differentiate, and further
319 underscores its pivotal role in the regulation of the two cell populations and their
320 progenies.

321 ESCs or TSCs are mostly cultivated in co-cultures with feeder cells that provide
322 them with nutrients and paracrine signals required for their cultivation. Our analyses show
323 that the regulation of ESC viability by lipid desaturases is less pronounced in co-culture
324 with MEFs than in feeder free culture, but still significant. This is likely due to the
325 differences in the media lipid composition, conferred by the feeder cells. We saw no effect
326 of D6D inhibition in TSCs in co-culture, implying that the advantage offered by inhibition
327 of polydesaturation is limited to their cultivation in feeder free culture.

328 Taken together, our data suggest that lipid polydesaturation is a common
329 metabolic signature of differentiating blastocyst-derived SCs, marking a shift from self-
330 renewal to differentiation. This shift is pro-apoptotic in both ESCs and TSCs via
331 downregulation of Scd1 in ESCs (dominant variant~35 kDa) whereas upregulation of
332 Scd1 (showing a ~63-70 kDa variant) in TSCs. Our results expand the concept of
333 metabolic regulation of stem cells fate decisions to the extra-embryonic stem cells, and
334 make a clear functional distinction between mono-and poly-desaturation of lipids in these
335 cells. Our work on blastocyst-derived cells suggests that the availability of MUFAs and
336 PUFAs in the microenvironment of the blastocyst, and the expression of D6D, D5D and
337 Scd1 in the blastocyst cell types are critical regulators of the concerted differentiation and
338 expansion of the blastocyst cell populations. Such premise requires further studies, and
339 especially in mammalian embryos.

340

341 **MATERIALS AND METHODS**

342 **Cell lines**

343 R1 *Oct4*-GFP ESCs were kindly provided by Prof. Andras Nagy of the Lunenfeld
344 Research Institute. V6.5 ESCs were kindly provided by Rudolf Jaenisch, MIT. TNGA
345 Nanog ESCs (with a background of 129 / black 6) and the blastocyst-derived TSC clones:
346 BD TSC 1 with a background of 129 / black 6, and BD TSC 2 with Homo BL6 background
347 were kindly provided by Dr. Yosef Buganim, Hebrew University of Jerusalem.

348 **Cell culture**

349 Cells were cultured in standard conditions. In brief: Cells were maintained in a humidified
350 incubator at 5% CO_2 and 37 °C (Thermo Fisher Scientific, USA).

351 ESCs in maintenance were cultured as previously described by us (17, 58), on a
352 confluent adhesive layer of mitomycin-inactivated MEF feeder cells in 2i ESC culture
353 DMEM medium supplemented with 15% Fetal bovine serum (FBS; Gibco, USA), 1.5%
354 Pen/Strep (Biological Industries,USA), 1% sodium pyruvate (Biological Industries, USA),
355 1% L-glutamine (Biological Industries, USA), 1% non-essential amino acids (Gibco, USA),
356 0.1 mM 2-mercaptoethanol (Gibco, USA), 2.8 μM CHIR99021 (Biogems, Peprotech), 1
357 μM PD0325901 (Biogems, Peprotech), mouse Leukemia inhibitory factor (LIF; in-house
358 production)]. Every two days, cells were passaged. Before experiments, ESCs were
359 cultured in feeder free conditions (in LIF/2i ESC culture medium) on 0.2% gelatin coated
360 culture plates for 3 passages.
361 TSCs in maintenance were cultivated as previously described (4), on gelatin
362 coated mitomycin inactivated MEFs in 30% TSC medium [RPMI 1640 (Gibco, USA)
363 supplemented with 20% FBS (Gibco, USA), 1% non-essential amino acids (Gibco, USA),
364 1% L-glutamine (Biological Industries, USA), 1% sodium pyruvate (Biological Industries,
365 USA), 1% pen/strep (Biological Industries, USA), 50 μM β-mercaptoethanol (Gibco,
366 USA)] and 70% MEF conditioned medium (medium collected from mitomycin inactivated
367 MEFs, containing the same supplements) freshly supplemented with 25 ng/mL of human
368 recombinant FGF4 (prepared in house) and 1 μg/mL heparin (Sigma-Aldrich, USA). TSCs
369 were passaged every 3-5 days, using trypsin EDTA. For feeder free experiments, TSCs
370 were cultured in Matrigel ® Matrix (Corning Life Sciences, USA) coated [1:30 dilution in
371 DMEM/F-12 medium (Gibco, USA)] tissue culture plates in Tx defined medium (59) with
372 freshly added 25 ng/mL of mouse recombinant FGF4 (In-house production), 1 μg/mL
373 heparin (Sigma-Aldrich, USA), 1 μg/mL of human TGFβ1 (Biogems, Peprotech).
374 Fetal bovine serum used throughout the study was from one batch, to avoid
375 possible batch-dependent changes in the lipid composition of the cultivation medium.
376 **ESC and TSC early differentiation**
377 Cells were cultivated in a feeder free medium: ESCs in 2i culture medium on 0.2% gelatin
378 coated plates and TSCs on Matrigel coated plates in TX defined medium (59). Cells were
379 maintained in feeder free conditions for at least 3 passages prior to experiments. For
380 initiation of differentiation, growth factors and cytokines that maintain cells in pluripotency
381 (LIF and 2i) or TSC state (heparin, recombinant human TGF-β and FGF-4) were excluded

382 from medium. For the infliction of differentiation, 24 hours following seeding, we allowed
383 SCs to differentiate by excluding the above factors from cultivation medium for 48 hours.
384 The medium of SCs of the same experimental lot was replaced with fresh ESC/TSC
385 culture medium as above, and they were used as undifferentiated control. We then
386 compared the metabolic composition of early differentiating SCs to that of undifferentiated
387 cells.

388 **Metabolomics analyses**

389 Following 0-48 hours of spontaneous differentiation, ESCs or TSCs were harvested and
390 centrifuged at 200 g, 4 °C, 5 min. Cell pellets were washed twice with Dulbecco's PBS
391 without Ca and Mg (Biological Industries, USA), snap frozen in liquid nitrogen, and kept
392 at -80 °C. Cell pellets were extracted in an ice cold solvent containing 86.5% methanol
393 (J. T. Baker, USA), 12.5% LC-MS grade water (J. T. Baker, USA), 1% formic acid (Tokyo
394 Chemical Industry Co., Ltd., Japan). Samples were vortexed and extracted by
395 ultrasonication followed by freeze-thaw cycles. Ultrasonication was carried out using
396 Bioruptor® Plus sonicator (Diagenode, USA) at 30 second on / off pulsation cycles for 5
397 min. Following centrifugation, ultra-sonication and freezing cycles were repeated for two
398 additional cycles and pooled for each sample in a fresh pre-labeled glass tube.
399 Supernatant was transferred to clean glass tubes, and concentrated in a SC210A speed
400 vacuum concentrator (SAVANT SPD 121P, Thermo scientific, USA) at 30 °C. The
401 remaining pellet was extracted in 400 µL acetone, ultra-sonicated for 30 seconds, and
402 centrifuged for 10 min at 4 °C. Supernatant was transferred to the respective glass tubes
403 containing the methanol/water concentrated extracts and concentrated to dryness.
404 Samples were reconstituted in 200 µL of reconstitution solvent: 95% acetonitrile (J. T
405 Baker, USA; LC-MS grade), 5% water (LC-MS grade; J. T Baker, USA), 0.1% formic acid
406 (Tokyo Chemical Industry Co., Ltd., Japan), and transferred to 96 well 700 µl sample plate
407 (Waters®Acquity UPLC plate, USA).

408 Ten microliters of samples were injected to a Waters Acquity UPLC H-Class apparatus
409 (Waters, Milford, MA, USA) equipped with UPLC CSH C18 2.1 x100 mm, 1.7 µm column
410 (Waters, Ireland). The column was equilibrated with 0.4 mL/min flow of 40% of mobile
411 phase A (ACN: Water 2:98% V/V) and 60% of mobile phase B (ACN). The linear gradient
412 program was as follows: 60% mobile phase A (0.1% formic acid in water) and 40% mobile

413 phase B for 1 min. The mobile phase B proportion was increased to 70% (v/v) in 5 min.
414 From 5 to 8 min, mobile phase consisted of 24% A, 40% B, and 36% C [(isopropanol
415 (Chemsolute, T.Geyer)]; from 8 to 9 min, 20% A, 35% B, and 45% C; from 9 to 12 min,
416 18.4% A, 33% B, and 48.6% C; from 12 to 17 min, 12% A, 25% B, and 63% C; and up to
417 25 min, 0.4% A, 10.5% B, and 89.1% C. Aquity UPLC system was coupled to a Xevo G2-
418 XS, high resolution and high mass accuracy QTOF equipped with ESI. Negative ion mode
419 was used for downstream analyses. Masses of 30-2000 Dalton underwent MS^E analysis
420 with ramp collision energies 30-60eV. Mass range calibration was performed using
421 Leucine enkephalin (Waters, USA) infused every 0.3 seconds. A quality control (QC) mix
422 prepared from pooled samples was injected every 10 runs. A blank sample was injected
423 every 10 samples. A minimum intensity cutoff mass was set to 100 m/z. Fold change
424 greater than 100 from blank and lowest mean abundance in blank was set as another
425 threshold. Data acquisition and visualization was performed using MassLynx 4.1 (Waters
426 Co., UK). Spectral deconvolution, alignment, and normalization were performed using
427 Progenesis QI (Nonlinear dynamics, Waters Corporation, UK). For metabolite
428 identification, exact mass, isotope patterns and fragmentation patterns were compared to
429 18 metabolite libraries compatible with Progenesis QI (60). Multivariate statistical
430 analyses, masses were carried out using Progenesis QI and Metaboanalyst 4.0 (Waters
431 Corporation, UK). Feature intensities were quantile normalized.
432 **Evaluation of total arachidonic acid levels using GC-MS.** ESCs or TSCs were
433 harvested and washed twice with PBS. Cell pellet ($1x10^6$ cells) was snap frozen in liquid
434 nitrogen and lyophilized (Labconco Corporation, USA). Lyophilized cell pellets were
435 hydrolyzed with 1mL of 1M KOH (Sigma Aldrich, USA) in 70% Ethanol (JT Baker, USA;
436 HPLC grade) at 90 °C for 1 hour. The reaction mixture was acidified with 0.2 mL of 6M
437 HCl (Sigma Aldrich, USA) and then 1 mL of water was added. The hydrolyzed fatty acids
438 were extracted with 1mL of hexane (GC grade, Sigma Aldrich, USA) and further
439 concentrated using vacuum concentrator (Savant SPD121P speed-vac concentrator,
440 Thermo Scientific, USA). Fatty acids were then methylated with 2 mL of Boron Trifluoride
441 (BF3) in Methanol (14% W/V) (Sigma Aldrich, USA) and incubated at 55 °C for 1.5 hours
442 with intermittent shaking every 20 min. 2 mL of saturated solution of $NaHCO_3$ (Sigma
443 Aldrich, USA) and 3 mL of hexane were then added, and the tubes were vortex-mixed for

444 a minute. The hexane layer was recovered carefully and concentrated using vacuum
445 concentrator. Samples were reconstituted in 100 µL hexane (GC grade, Sigma Aldrich,
446 USA). GC-MS analysis was performed using an Agilent 8860 GC system equipped with
447 an Agilent 7683 N auto sampler and a Agilent J& W GC columns
448 (30 m × 0.25 mm × 0.2 µm, Agilent technologies USA). The injector was set at 220 °C and
449 1 µL injections were made with helium as carrier gas, maintained at flow rate of 1 mL/min.
450 GC gradient is given as **Table S2**. The transfer line from GC column to MS (Agilent 5977B
451 GC/MSD) was set to 250 °C, ionization energy of 70 eV. A standard for arachidonic acid
452 (Sigma Aldrich, USA) was used for validation of identification.

453 **Scd1 or D6D enzyme inhibition assay**

454 Selective inhibitors for Scd1 PluriSIn-1 and A-939572, D6D (SC-26196) and D5D
455 (sesamin) were purchased from Cayman Chemicals, USA. The effect of the
456 pharmacological inhibitors was evaluated for ESCs and TSCs following 48 hours
457 incubation. Oleate conjugated to albumin (Sigma Aldrich, USA) was also tested for its
458 influence on Scd1 or D6D-inhibited TSCs.

459 **SiRNA transfection**

460 ESCs were maintained at a density of 2.5 x 10^4 cells/well in 24 well plate for 24 hours
461 following passage, in ESC LIF/2i medium. Cells were transfected with MISSION® SiRNA
462 oligomers or MISSION® siRNA Universal Negative Control #1 (Sigma Aldrich, Merck,
463 USA) at a final concentration 20 nM, mixed with 1.5 µL X-tremeGENE transfection
464 reagent (Sigma Aldrich, Merck, USA). The complex was incubated at room temperature
465 for 30 min in serum free medium and transferred to the cells. Following 6 hours post
466 transfection, the medium was replaced with ESC LIF/2i medium, and the cells were
467 harvested after 48 hours.

468 **Cell counts**

469 Cells were seeded at a density of 15,000 (ESCs) or 50,000 (TSCs) cells per well in 24
470 well plates, in feeder free culture. Cell count was carried out using Cyto Smart cell counter
471 (Corning Incorporated Life Sciences, USA). Counts were validated by manual counting.

472 **Fluorescent Detection**

473 Fluorescence of *Oct4*-GFP ESCs was further quantified using CYTATION 3 plate reader
474 (LUMITRON, Israel) at an excitation wavelength of 395 nm and emission peak of 509 nm.

475 **Microscopy**

476 Microscopic imaging was taken at 10 x magnification using OLYMPUS IX73 Inverted
477 Microscope (OLYMPUS Life Science, USA).

478 **Quantitative real-time Polymerase Chain Reaction (RT qPCR)**

479 Total RNA for the experiments was extracted from the cells using GENEzol™ TriRNA
480 Pure Kit + DNAse (Geneaid HyLabs, Taiwan) according to the manufacturer's protocol.
481 Quantification of total RNA concentration was done using NanoDrop ND-1000
482 spectrophotometer (Version 3.8.1, Thermo Fisher). First strand cDNA synthesis was done
483 from 1000 ng of RNA using qScript cDNA Synthesis kit (Quantabio, USA). RT qPCR was
484 performed using Fast SYBR™ Green Master Mix (Applied Biosystems™, Thermo Fisher)
485 and a CFX Connect™ Real-Time PCR Detection System. Primer sequences (HyLabs
486 and IDT) are listed in **Table S3**. Relative expression of the transcripts was normalized to
487 Hypoxanthine Phosphoribosyltransferase (HPRT)1 or Ubiquitin C (UBC), and the gene
488 expression was quantified based on comparative $2^{-\Delta\Delta CT}$.

489 **Flow cytometry**

490 Following dissociation, cells were centrifuged at 200 g for 5 min, and cell pellets were
491 washed twice in PBS containing 1% FBS, and filtered through a cell strainer to remove
492 aggregates. Cells incubated with secondary and no primary antibody (for stained cells) or
493 unlabeled cells (for GFP-labeled cells) were used as negative controls. Flow cytometry
494 was carried out on CytoFLEX Flow Cytometer (BECKMAN COULTER, Life Sciences)
495 using a 100 µm nozzle. Analysis was carried out using CytExpert 2.4 software
496 (BECKMAN COULTER, Life Sciences). For TSCs in co-culture with feeder cells, cells
497 were incubated with anti-CD40 antibody (Ab22469, 1:300; Abcam), and then with Alexa
498 Flour-conjugated anti Rat 488 secondary antibody (Ab150153, 1:500; Abcam).

499 **Apoptosis assay**

500 Cells were seeded on 0.2% gelatin (ESCs) or matrigel (1:30 dilution; TSCs) coated culture
501 plates. Cell pellets were washed with ice cold PBS and resuspended in 1X Annexin V
502 binding buffer (Cell Signaling Technology, USA). Cells were then incubated with Annexin
503 V-FITC conjugate (Cell Signaling Technology, USA) for 10 min on ice protected from light.
504 Propidium Iodide (20 µg/mL; Fisher Scientific, USA) was added to cell suspension
505 immediately before FACS analysis.

506 **Immunoblotting**

507 Cells were collected by trypsinization, then washed with PBS (Biological Industries,
508 Israel). Proteins were extracted with 100 µL in-house made RIPA (1% NP-40, 0.1%SDS,
509 1M Tris-HCL pH 7.4, NaCl, Sodium deoxycholate, EDTA, and water) + Protease Inhibitors
510 (Roche, USA) and quantified using Bradford reagents (Sigma Aldrich, USA). Extracted
511 proteins were reconstituted in an in-house Protein Sample Buffer (Glycerol 100%, 1M Tris
512 pH6.8, 10% SDS, β- mercaptoethanol, bromophenol blue) and heated for 10 min at 95
513 °C. Proteins were separated on 10% SDS-PAGE gels and transferred to 0.22 µm PVDF
514 membrane (FroggaBio, USA) by an electric current at 300 mA for 70 min. The membrane
515 was blocked in 5% BSA/TBST for 2 hours, then incubated with primary antibody
516 overnight. Scd1 antibody was purchased from Cell Signaling Technology USA, (#2794,
517 1:1,000). Membrane was washed, then incubated with HRP conjugated secondary
518 antibody (Abcam, USA, Ab 6721, 1:10,000). eIF4G2/p97 antibody from Cell Signaling
519 Technology (#2182, 1: 3000), or mouse monoclonal anti α-tubulin antibody (T5168;
520 Sigma Aldrich, USA) were used as a loading control. Chemiluminescence was detected
521 by ECL (Advansta, USA), using Molecular Imager ChemiDoc™ XRS (Bio-Rad, USA).

522 **Cell cycle analysis**

523 Cells were seeded at a density of 30,000 (ESCs) or 100,000 (TSCs) cells per well in a 6
524 well culture plate and treated with D6D inhibitor or DMSO vehicle for 24 hours. Upon 70%
525 cell confluence, cells were treated with 10 µM of Edu (5-ethynyl-2′ -deoxyuridine;
526 Invitrogen™, Thermo Fisher Scientific, USA), and incubated for 30 min. After labeling,
527 cells were harvested and washed twice with PBS. Cell pellets were resuspended in cold
528 PBS and fixed by adding cold absolute ethanol dropwise while mixing. Cells were
529 incubated overnight at 4 °C. Following centrifugation, cell pellets were permeabilized by
530 adding 0.1% Triton® X-100 (Sigma Aldrich, USA) in PBS [1% BSA (Sigma Aldrich, USA)],
531 and stained with Click-iT reaction mix [50 mM Trizma® Hydrochloride Buffer pH 7.5
532 (Sigma Aldrich, USA), 150 mM NaCL (Sigma Aldrich, USA), 2 mM CuSO4 (Sigma
533 Aldrich), 2.5 µM Alexa Fluor 647 azide triethyl ammonium salt in DMSO (Thermo Fisher
534 Scientific, USA) and 10 mM Sodium ascorbate (Sigma Aldrich, USA)] for 30 min. The
535 cells were again washed with 0.1% Triton® X-100, 1% BSA in PBS, and stained with
536 propidium iodide (Thermo Fisher Scientific, USA), 50 µg/mL of RNase (Thermo Fisher

537 Scientific, USA) in PBS. EdU-analysis was performed using CytoFLEX Flow Cytometer
538 and CytExpert 2.4 software (BECKMAN COULTER, Life Sciences).
539
540
541 **REFERENCES**

542 .1 Sozen B, Cox AL, De Jonghe J, Bao M, Hollfelder F, Glover DM, et al. Self-Organization
543 of Mouse Stem Cells into an Extended Potential Blastoid. Dev Cell. 2019;51(6):698-712 e8.
544 .2 Shyh-Chang N, Daley GQ, Cantley LC. Stem cell metabolism in tissue development and
545 aging. Development. 2013;140(12):2535-47.
546 .3 Blair K, Wray J, Smith A. The liberation of embryonic stem cells. PLoS Genet.
547 2011;7(4):e1002019.
548 .4 Benchetrit H, Herman S, van Wietmarschen N, Wu T, Makedonski K, Maoz N, et al.
549 Extensive Nuclear Reprogramming Underlies Lineage Conversion into Functional Trophoblast
550 Stem-like Cells. Cell Stem Cell. 2015;17(5):543-56.
551 .5 Shahbazi MN, Zernicka-Goetz M. Deconstructing and reconstructing the mouse and
552 human early embryo. Nat Cell Biol. 2018;20(8):878-8.7
553 .6 Rossant J, Tam PPL. Opportunities and challenges with stem cell-based embryo models.
554 Stem Cell Reports. 2021;16(5):1031-8.
555 .7 Moussaieff A, Rouleau M, Kitsberg D, Cohen M, Levy G, Barasch D, et al. Glycolysis-
556 mediated changes in acetyl-CoA and histone acetylation control the early differentiation of
557 embryonic stem cells. Cell Metab. 2015;21(3):392-402.
558 .8 Panopoulos AD, Yanes O, Ruiz S, Kida YS, Diep D, Tautenhahn R, et al. The metabolome
559 of induced pluripotent stem cells reveals metabolic changes occurring in somatic cell
560 reprogramming. Cell Res. 2012;22(1):168-77.
561 .9 Yanes O, Clark J, Wong DM, Patti GJ, Sanchez-Ruiz A, Benton HP, et al. Metabolic
562 oxidation regulates embryonic stem cell differentiation. Nat Chem Biol. 2010;6(6):411-7.
563 .10 Sperber H ,Mathieu J, Wang Y, Ferreccio A, Hesson J, Xu Z, et al. The metabolome
564 regulates the epigenetic landscape during naive-to-primed human embryonic stem cell transition.
565 Nat Cell Biol. 2015;17(12):1523-35.

566 .11 Shiraki N, Shiraki Y, Tsuyama T, Obata F, Miura M, Nagae G, et al. Methionine
567 metabolism regulates maintenance and differentiation of human pluripotent stem cells. Cell Metab.
568 2014;19(5):780-94.
569 .12 Park H, Haynes CA, Nairn AV, Kulik M, Dalton S, Moremen K, et al. Transcript profiling
570 and lipidomic analysis of ceramide subspecies in mouse embryonic stem cells and embryoid
571 bodies. J Lipid Res. 2010;51(3):480-9.
572 .13 Ito K, Suda T. Metabolic requirements for the maintenance of self-renewing stem cells.
573 Nat Rev Mol Cell Biol. 2014;15(4):243-56.
574 .14 Carey BW, Finley LW, Cross JR, Allis CD, Thompson CB. Intracellular alpha-
575 ketoglutarate maintains the pluripotency of embryonic stem cells. Nature. 2015;518(7539):413-6.
576 .15 Cezar GG, Quam JA, Smith AM, Rosa GJ, Piekarczyk MS, Brown JF, et al. Identification
577 of small molecules from human embryonic stem cells using metabolomics. Stem Cells Dev.
578 2007;16(6):869-82.
579 .16 Chung S, Dzeja PP, Faustino RS, Perez-Terzic C, Behfar A, Terzic A. Mitochondrial
580 oxidative metabolism is required for the cardiac differentiation of stem cells. Nat Clin Pract
581 Cardiovasc Med. 2007;4 Suppl 1:S60-7.
582 .17 Elena-Herrmann B, Montellier E, Fages A, Bruck-Haimson R, Moussaieff A. Multi-
583 platform NMR Study of Pluripotent Stem Cells Unveils Complementary Metabolic Signatures
584 towards Differentiation. Sci Rep. 2020;10(1):1622.
585 .18 Folmes CD, Dzeja PP, Nelson TJ, Terzic A. Metabolic plasticity in stem cell homeostasis
586 and differentiation. Cell Stem Cell. 2012;11(5):596-606.
587 .19 Folmes CD, Nelson TJ, Martinez-Fernandez A, Arrell DK, Lindor JZ, Dzeja PP, et al.
588 Somatic oxidative bioenergetics transitions into pluripotency-dependent glycolysis to facilitate
589 nuclear reprogramming. Cell Metab. 2011;14(2):264-71.
590 .20 Gu W, Gaeta X, Sahakyan A, Chan AB, Hong CS, Kim R, et al. Glycolytic Metabolism
591 Plays a Functional Role in Regulating Human Pluripotent Stem Cell State. Cell Stem Cell.
592 2016;19(4):476-90.
593 .21 Han S, Auger C, Thomas SC, Beites CL, Appanna VD. Mitochondrial biogenesis and
594 energy production in differentiating murine stem cells: a functional metabolic study. Cell
595 Reprogram. 2014;16(1):84-90.

596 .22 Maury JJ, Chan KK, Zheng L, Bardor M, Choo AB. Excess of O-linked N-
597 acetylglucosamine modifies human pluripotent stem cell differentiation. Stem Cell Res.
598 2013;11(2):926-37.
599 .23 Moussaieff A, Kogan NM, Aberdam D. Concise Review: Energy Metabolites: Key
600 Mediators of the Epigenetic State of Pluripotency. Stem Cells. 2015;33(8):2374-80.
601 .24 TeSlaa T, Chaikovsky AC, Lipchina I, Escobar SL, Hochedlinger K, Huang J, et al. alpha-
602 Ketoglutarate Accelerates the Initial Differentiation of Primed Human Pluripotent Stem Cells. Cell
603 Metab. 2016;24(3):485-93.
604 .25 Teslaa T, Teitell MA. Pluripotent stem cell energy metabolism: an update. EMBO J.
605 2015;34(2):138-53.
606 .26 Prigione A, Fauler B, Lurz R, Lehrach H, Adjaye J. The senescence-related
607 mitochondrial/oxidative stress pathway is repressed in human induced pluripotent stem cells. Stem
608 Cells. 2010;28(4):721-33.
609 .27 Shyh-Chang N, Locasale JW, Lyssiotis CA, Zheng Y, Teo RY, Ratanasirintrawoot S, et
610 al. Influence of threonine metabolism on S-adenosylmethionine and histone methylation. Science.
611 2013;339(6116):222-6.
612 .28 Teslaa T, Teitell MA. Pluripotent stem cell energy metabolism: an update. EMBO J. 2014.
613 .29 Wang J, Alexander P, Wu L, Hammer R, Cleaver O, McKnight SL .Dependence of mouse
614 embryonic stem cells on threonine catabolism. Science. 2009;325(5939):435-9.
615 .30 Lu C, Thompson CB. Metabolic regulation of epigenetics. Cell Metab. 2012;16(1):9-17.
616 .31 Zhang H, Badur MG, Divakaruni AS, Parker SJ, Jager C, Hiller K ,et al. Distinct Metabolic
617 States Can Support Self-Renewal and Lipogenesis in Human Pluripotent Stem Cells under
618 Different Culture Conditions. Cell Rep. 2016;16(6):1536-47.
619 .32 Jang H, Kim TW, Yoon S, Choi SY, Kang TW, Kim SY, et al. O-GlcNAc regulates
620 pluripotency and reprogramming by directly acting on core components of the pluripotency
621 network. Cell Stem Cell. 2012;11(1):62-74.
622 .33 Kleger A, Busch T, Liebau S, Prelle K, Paschke S, Beil M, et al. The bioactive lipid
623 sphingosylphosphorylcholine induces differentiation of mouse embryonic stem cells and human
624 promyelocytic leukaemia cells. Cell Signal. 2007;19(2):367-77.

625 .34 Prigione A, Adjaye J. Modulation of mitochondrial biogenesis and bioenergetic
626 metabolism upon in vitro and in vivo differentiation of human ES and iPS cells. Int J Dev Biol.
627 2010;54(11-12):1729-41.
628 .35 Lin N, Qin S, Luo S, Cui S, Huang G, Zhang X. Homocysteine induces cytotoxicity and
629 proliferation inhibition in neural stem cells via DNA methylation in vitro. FEBS J.
630 2014;281(8):2088.96-
631 .36 Kondoh H, Lleonart ME, Nakashima Y, Yokode M, Tanaka M, Bernard D, et al. A high
632 glycolytic flux supports the proliferative potential of murine embryonic stem cells. Antioxid Redox
633 Signal. 2007;9(3):293-9.
634 .37 Ben-David U, Gan QF, Golan-Lev T, Arora P, Yanuka O, Oren YS, et al. Selective
635 elimination of human pluripotent stem cells by an oleate synthesis inhibitor discovered in a high-
636 throughput screen. Cell Stem Cell. 2013;12(2):167-79.
637 .38 Zhang J, Nuebel E, Daley GQ, Koehler CM, Teitell MA. Metabolic regulation in
638 pluripotent stem cells during reprogramming and self-renewal. Cell Stem Cell. 2012;11(5):589-
639 95.
640 .39 Zhu S, Li W, Zhou H, Wei W, Ambasudhan R, Lin T, et al. Reprogramming of human
641 primary somatic cells by OCT4 and chemical compounds. Cell Stem Cell. 2010;7(6):651-5.
642 .40 Sturmey RG, Reis A, Leese HJ, McEvoy TG. Role of fatty acids in energy provision during
643 oocyte maturation and early embryo development. Reprod Domest Anim. 2009;44 Suppl 3:50-8.
644 .41 Garcia-Gonzalo FR, Izpisua Belmonte JC. Albumin-associated lipids regulate human
645 embryonic stem cell self-renewal. PLoS One. 2008;3(1):e1384.
646 .42 Wu Y, Chen K, Xing G, Li L, Ma B, Hu Z, et al. Phospholipid remodeling is critical for
647 stem cell pluripotency by facilitating mesenchymal-to-epithelial transition. Sci Adv.
648 2019;5(11):eaax7525.
649 .43 Radzisheuskaya A, Chia Gle B, dos Santos RL, Theunissen TW, Castro LF, Nichols J, et
650 al. A defined Oct4 level governs cell state transitions of pluripotency entry and differentiation into
651 all embryonic lineages. Nat Cell Biol. 2013;15(6):579-90.
652 .44 Latos PA, Sienerth AR, Murray A, Senner CE, Muto M, Ikawa M, et al. Elf5-centered
653 transcription factor hub controls trophoblast stem cell self-renewal and differentiation through
654 stoichiometry-sensitive shifts in target gene networks. Genes Dev. 2015;29(23):2435-48.

655 .45 Stanley EG, Jenkins BJ, Walker CG, Koulman A, Browning L, West AL, et al. Lipidomics
656 Profiling of Human Adipose Tissue Identifies a Pattern of Lipids Associated with Fish Oil
657 Supplementation .J Proteome Res. 2017;16(9):3168-79.
658 .46 Tabas I, Ron D. Integrating the mechanisms of apoptosis induced by endoplasmic
659 reticulum stress. Nat Cell Biol. 2011;13(3):184-90.
660 .47 Kim SJ, Zhang Z, Saha A, Sarkar C, Zhao Z, Xu Y, et al. Omega-3 and omega-6 fatty acids
661 suppress ER- and oxidative stress in cultured neurons and neuronal progenitor cells from mice
662 lacking PPT1. Neurosci Lett. 2010;479(3):292-6.
663 .48 Jakobsen CH, Storvold GL, Bremseth H, Follestad T, Sand K, Mack M, et al. DHA induces
664 ER stress and growth arrest in human colon cancer cells: associations with cholesterol and calcium
665 homeostasis. J Lipid Res. 2008;49(10):2089-100.
666 .49 Serini S, Piccioni E, Merendino N, Calviello G. Dietary polyunsaturated fatty acids as
667 inducers of apoptosis: implications for cancer. Apoptosis. 2009;14(2):135-52.
668 .50 Ntambi JM. Regulation of stearoyl-CoA desaturase by polyunsaturated fatty acids and
669 cholesterol. J Lipid Res. 1999;40(9):1549-58.
670 .51 Sampath H, Ntambi JM. Polyunsaturated fatty acid regulation of gene expression. Nutr
671 Rev. 2004;62(9):333-9.
672 .52 Sessler AM, Kaur N, Palta JP, Ntambi JM. Regulation of stearoyl-CoA desaturase 1 mRNA
673 stability by polyunsaturated fatty acids in 3T3-L1 adipocytes. J Biol Chem. 1996;271(47):29854-
674 8.
675 .53 Grandjean JMD, Madhavan A ,Cech L, Seguinot BO, Paxman RJ, Smith E, et al.
676 Pharmacologic IRE1/XBP1s activation confers targeted ER proteostasis reprogramming. Nat
677 Chem Biol. 2020;16(10):1052-61.
678 .54 Volmer R, van der Ploeg K, Ron D. Membrane lipid saturation activates endoplasmic
679 reticulum unfolded protein response transducers through their transmembrane domains. Proc Natl
680 Acad Sci U S A. 2013;110(12):4628-33.
681 .55 Zhang S, Yang Y, Shi Y. Characterization of human SCD2, an oligomeric desaturase with
682 improved stability and enzyme activity by cross-linking in intact cells. Biochem J. 2005;388(Pt
683 1):135-42.

684 .56 Fernandez Gianotti T, Burgueno A, Gonzales Mansilla N, Pirola CJ, Sookoian S. Fatty
685 liver is associated with transcriptional downregulation of stearoyl-CoA desaturase and impaired
686 protein dimerization. PLoS One. 2013;8(9):e76912.
687 .57 Flowers MT, Ntambi JM. Role of stearoyl-coenzyme A desaturase in regulating lipid
688 metabolism. Curr Opin Lipidol. 2008;19(3):248-56.
689 .58 Moussaieff A, Rogachev I, Brodsky L, Malitsky S, Toal TW, Belcher H, et al. High-
690 resolution metabolic mapping of cell types in plant roots. Proc Natl Acad Sci U S A.
691 2013;110(13):E1232-41.
692 .59 Kubaczka C, Senner C, Arauzo-Bravo MJ, Sharma N, Kuckenberg P, Becker A, et al.
693 Derivation and maintenance of murine trophoblast stem cells under defined conditions. Stem Cell
694 Reports. 2014;2(2):232-42.
695 .60 Shehadeh A, Bruck-Haimson R, Saidemberg D, Zacharia A, Herzberg S, Ben-Meir A, et
696 al. A shift in follicular fluid from triacylglycerols to membrane lipids is associated with positive
697 pregnancy outcome. FASEB J. 2019;33(9):10291-9.
698

699 **ACKNOWLEDGEMENTS**
700 We thank Dr. Yosef (Yossi) Buganim for the kind gift of blastocyst isolated TSCs and
701 ESCs and for providing the knowhow of TSC maintenance, and Abraham Greenberg and
702 Prof. Itamar Simon for their kind help with the cell cycle analysis.
703

704 **CONFLICT OF INTERESTS**
705 The authors declare no competing interests.
706

707 **AUTHOR CONTRIBUTIONS**
708 A.M. conceived the project, supervised the project, analyzed data, secured funding, and
709 wrote the manuscript. C.T.M. and R.B.H. maintained cell cultures and performed
710 experiments, A.S. maintained cell cultures, P.O. performed experiments. A.D. assisted in
711 preparing samples for analyses. A.Z., D.S., N.M.K., R.S. and S.A. analyzed data, I.P.
712 validated the effect of D6D inhibition on a second line of ESCs. A.M. and C.T.M. prepared
713 the manuscript for submission.
714

715 **ETHICS APPROVAL AND CONSENT TO PARTICIPATE**

716 This study did not require ethical approval.

717

718 **FUNDING**

719 This study was supported by The Dr. Adolf and Klara Brettler Center for Research in
720 Molecular Pharmacology and Therapeutics.

721

722 **DATA AVAILABILITY STATEMENT**

723 The datasets used and/or analyzed during the current study are available from the
724 corresponding author on reasonable request.

725

726 **FIGURE LEGENDS**

727 **Figure 1.**

728 **The metabolism of blastocyst-derived SCs shifts upon early differentiation.** ESCs
729 and TSCs (0.5 x 10^6 cells per sample) were seeded in the culture media commonly used
730 for their maintenance (Materials and Methods). After 24 hours, medium was changed to
731 fresh medium with ("Undiff") or without ("Early Diff") factors that support self-renewal.
732 ESCs were allowed to differentiate by the exclusion of LIF and 2i from cell medium. The
733 colonies of early differentiating ESCs show a non-condensed, non-organized morphology
734 (A). Early differentiating ESCs of the experimental lot used for the metabolomics analysis
735 were evaluated for the expression of pluripotency markers by RT q-PCR (B). Following
736 quantile normalization of the data, partial least squares discriminant analyses (PLS-DA)
737 of early differentiating vs undifferentiated ESCs was performed. R^2=0.89, Q^2 = 0.69 for
738 hetero agouti (HA) blastocyst derived ESCs (BD ESCs); R^2 = 0.93, Q^2 = 0.84 for TNGA
739 *Nanog* ESCs (C). TSCs were allowed to differentiate by the exclusion of FGF4 and
740 heparin from cell medium. The colonies of early differentiating TSCs show a non-
741 condensed non-organized morphology (D). The expression of TSC marker genes upon
742 early differentiation was evaluated by RT q-PCR (E). Following quantile normalization of
743 the data, PLS-DA of early differentiating vs undifferentiated TSCs. R^2 = 0.99, Q^2 = 0.98
744 for blastcyst derived (BD TSC 1, R^2 = 0.99, Q^2 = 0.91 for BD TSC 2 (F). Values are the
745 mean ± SEM. n=6. *, P < 0.05; *, P < 0.01; **.

746

747 **Figure 2. Polyunsaturated lipids are a metabolic signature of early differentiating**
748 **ESCs and TSCs.** ESCs and TSCs of the same background (129 / black 6) were seeded
749 in Tx defined culture medium. After 24 hours, medium was changed to fresh medium with
750 ("Undiff") or without ("Early Diff") factors that support self-renewal. Their metabolome was
751 examined after 48 hours, using 0.5 x 10^6 cells per sample. The second principal
752 component (PC2) of a partial least squares discriminant analysis (PLS-DA; A) shows
753 discrete metabolome of the differentiating SCs. $R^2 = 0.93$, $Q^2 = 0.83$ (n = 6). A heat map
754 representation of the abundance of identified differential polyunsaturated phospholipids
755 of the dataset shown in A, following variable importance in projection (VIP; > 1) analysis
756 (B). The abundance of each metabolic feature was normalized to the sum intensity of
757 peaks of each chromatogram. The colors of quadrants in the heat maps represent the
758 relative abundance of the metabolites, after normalization to the mean abundance of each
759 metabolite across all samples (n = 6). Following hydrolysis of lipids in ESC extracts, total
760 abundance of linoleic acid (C) and arachidonic acid (D) was measured by GC-MS and
761 normalized to the sum of peaks area. The biosynthesis of PUFAs starts from essential
762 fatty acids with two double bonds, and is catalyzed by D6D and D5D (E). *D6D* and *D5D*
763 expression is upregulated in early differentiating ESCs (F) and TSCs (G), as measured
764 by RT-PCR (n = 6). ESCs and TSCs (129 / black 6 background) were treated by the D6D
765 inhibitor SC-26196 (0.2 μM) or DMSO control for 48 hours in feeder free culture without
766 2i/LIF or FGF4/TGFβ/heparin and the expression of stem cell markers was measured by
767 RT-qPCR (H-I; n = 4). Values are the mean ± SEM. *, $P < 0.05$; **, $P < 0.01$; ***, $P <$
768 0.001.

769

770 **Figure 3. Polydesaturation of lipids causes ER stress-related apoptosis in ESCs.**
771 ESCs (129 / black 6 background in A-I; V6.5 in J-K) were treated with the specific D6D
772 inhibitor SC-26196 (0.2 μM), D5D inhibitor sesamin (10 μM), or DMSO control for 48
773 hours in feeder free culture. Cell counting was carried out using CytoSmart cell counter
774 and validated by manual counting (A; n = 4). Fluorescence was quantified in *Oct4*-GFP
775 labeled 129 / black 6 ESCs using a plate reader to verify the increase in proliferation (B;
776 n = 4). Colony numbers per field were estimated under the microscope (C; 5 fields taken

777 for each well, for 4 wells). Cell survival was further evaluated by a clonogenicity assay (D;
778 (n = 48). Cell count was further carried out in defined Tx medium (E; n = 4). Dose response
779 evaluation of the influence of D6D inhibition on cell proliferation rate was performed with
780 0.1-3 μM SC-26196 (F; n = 4). For validation of the specific effect on D6D, siRNA was
781 applied (G; n = 4). The expression of the ER stress activators *IRE1*, *ATF6*, and *ASP* was
782 assessed by RT-qPCR upon D6D inhibition for 24 hours (H; n = 4). The percentage of
783 dead cells in D6D inhibited ESCs was further assessed by propidium iodide (PI) staining
784 (I; n = 4). To evaluate apoptosis in V6.5 ESCs (as they have no GFP label) following 24
785 hours of D6D inhibition, we used a kit based on annexin V-FITC staining. A representative
786 dot plot and the corresponding bar graph of one of four experiments (n = 4 for each) is
787 presented (J-K). Data are presented as mean ± SEM. *, P < 0.05; **, P < 0.01; ***, P <
788 0.001.
789
790 **Figure 4. D6D causes ER stress-related apoptosis and modifies cell cycle in TSCs.**
791 TSCs (129 / black 6) were treated by SC-26196 (0.2 μM) or DMSO control for 48 hours
792 in feeder free culture. Cell counting was carried out using CytoSmart cell counter and
793 validated by manual counting (A; n = 4). Colony numbers per field were estimated under
794 the microscope (B; 5 fields taken for each well, for 4 wells). The expression of *IRE1*, *ATF6*
795 and *ASP* was examined by RT-qPCR following D6D inhibition for 24 h (C; n = 4).
796 Apoptosis was assessed in TSCs following D6D inhibition for 24 hours using Annexin
797 V/PI staining (D-E; n = 4). The numbers in each quadrant of dot plot represent the
798 percentage of cells. Cell cycle was analyzed following inhibition of D6D by SC-26196 for
799 24 hours. The numbers in each quadrant of dot plot represent the percentage of cells (F-
800 G; n = 4). Data are presented as mean ± SEM. *, P < 0.05; ***, P < 0.001.
801
802 **Figure 5. D6D regulates Scd1 expression, essential for ESCs, but deleterious for**
803 **TSCs.** The expression of *Scd1* in feeder free culture following 48 hours of inhibition of
804 D6D (0.2 μM SC-26196), or in DMSO-treated control cells, was evaluated by RT-qPCR
805 in undifferentiated ESCs (A) and TSCs (B) (both 129 / black 6 background). *Scd1*
806 expression was also assessed in early differentiating ESCs and TSCs, compared to their
807 undifferentiated counterparts (C). The influence of Scd1 on pluripotency (D) or TSC (E)

808 markers in early differentiating SCs, as well as on cell viability (F-J) was evaluated
809 following treatment with Scd1 inhibitors [PluriSIn 1 (20 μM) or A939571 (300 nM)] or
810 DMSO vehicle for 48 hours. Conjugated oleate (100 μM) was added to PluriSin 1-treated
811 TSC culture (J). The expression of *IRE1*α, *ATF3*, *ATF6*, and *ASP* was assessed by RT-
812 qPCR following inhibition of Scd1 by PluriSIn 1 for 48 hours (K), and concomitant
813 apoptosis was evaluated using an Annexin V-FITC-based kit (L-M). The relative
814 expression of *Scd1* in self-renewing ESCs and TSCs was evaluated by RT-qPCR (N).
815 Monounsaturated fatty acyl chain phospholipids were identified and quantified in self-
816 renewing TSCs and ESCs by LC-MS. The abundance of each metabolic feature was
817 normalized to the sum intensity of peaks of each chromatogram. The colors of quadrants
818 in the heat maps represent the relative abundance of the metabolites, after normalization
819 to the mean abundance of each metabolite across all samples (n = 6; O). Scd1 protein
820 expression was determined by Western blot analysis (10% acrylamide gel) in self-
821 renewing ESCs and TSCs in ESC cultivation medium or Tx medium, respectively (P), or
822 both cell types in the same defined Tx medium (Q). TSC proliferation was evaluated in
823 TSCs, as above, following incubation with PluriSIn 1 or PluriSIn 1+conjugated oleate (100
824 μM) (n = 4; R). Data are presented as mean ± SEM. n=4. *, $P < 0.05$; **, $P < 0.01$; ***, P
825 < 0.001.

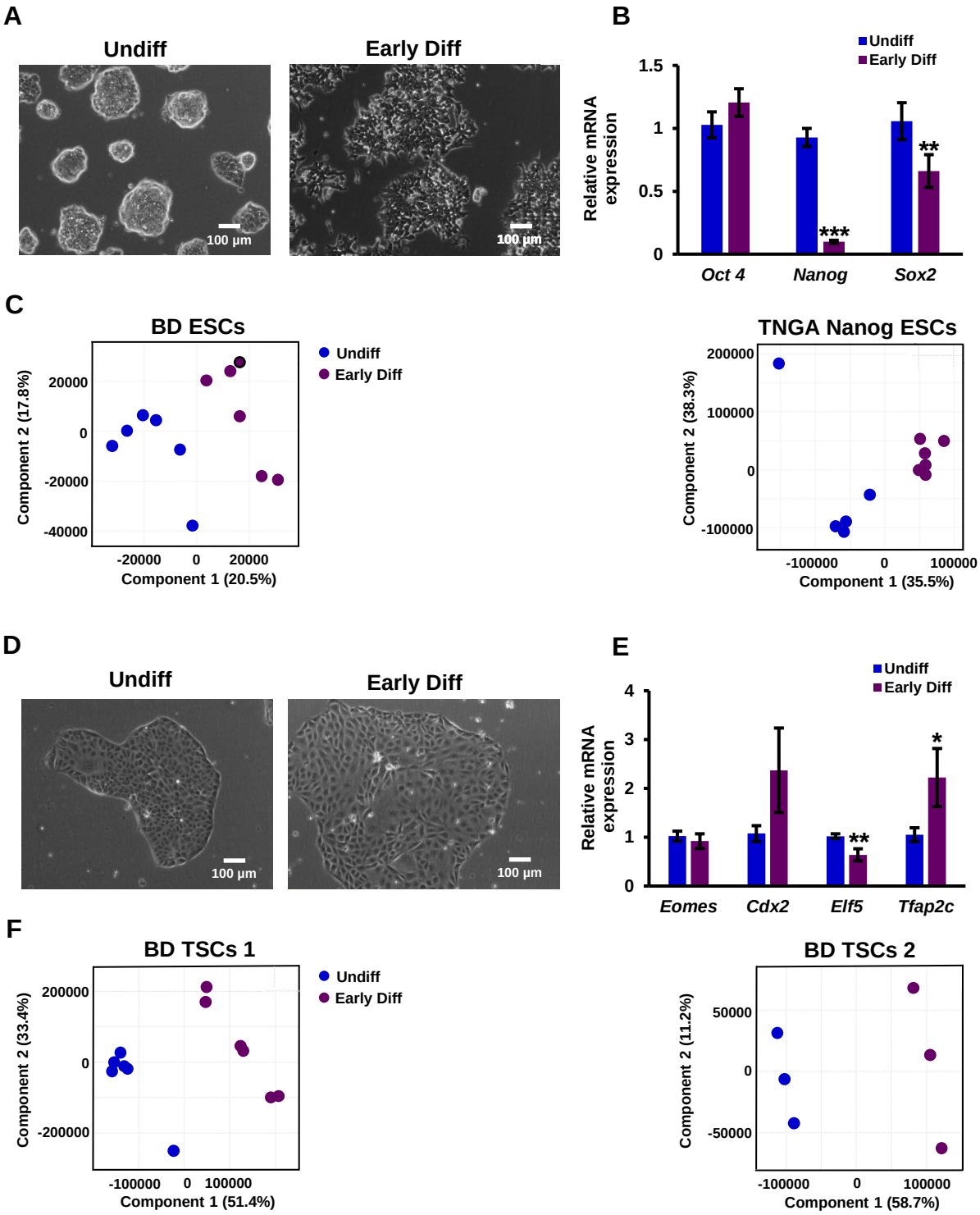
A
Undiff
Early Diff
100 µm
100 µm
B
Undiff
Early Diff
Relative mRNA expression
1.5
1
0.5
0
***
**
Oct 4
Nanog
Sox2
C
BD ESCs
Undiff
Early Diff
Component 2 (17.8%)
20000
0
-20000
-40000
-20000
0
20000
Component 1 (20.5%)
TNGA Nanog ESCs
Component 2 (38.3%)
200000
100000
0
-100000
-100000
0
100000
Component 1 (35.5%)
D
Undiff
Early Diff
100 µm
100 µm
E
Undiff
Early Diff
Relative mRNA expression
4
3
2
1
0
*
**
Eomes
Cdx2
Elf5
Tfap2c
F
BD TSCs 1
Undiff
Early Diff
Component 2 (33.4%)
200000
0
-200000
-100000
0
100000
Component 1 (51.4%)
BD TSCs 2
Component 2 (11.2%)
50000
0
-50000
-100000
0
100000
Component 1 (58.7%)

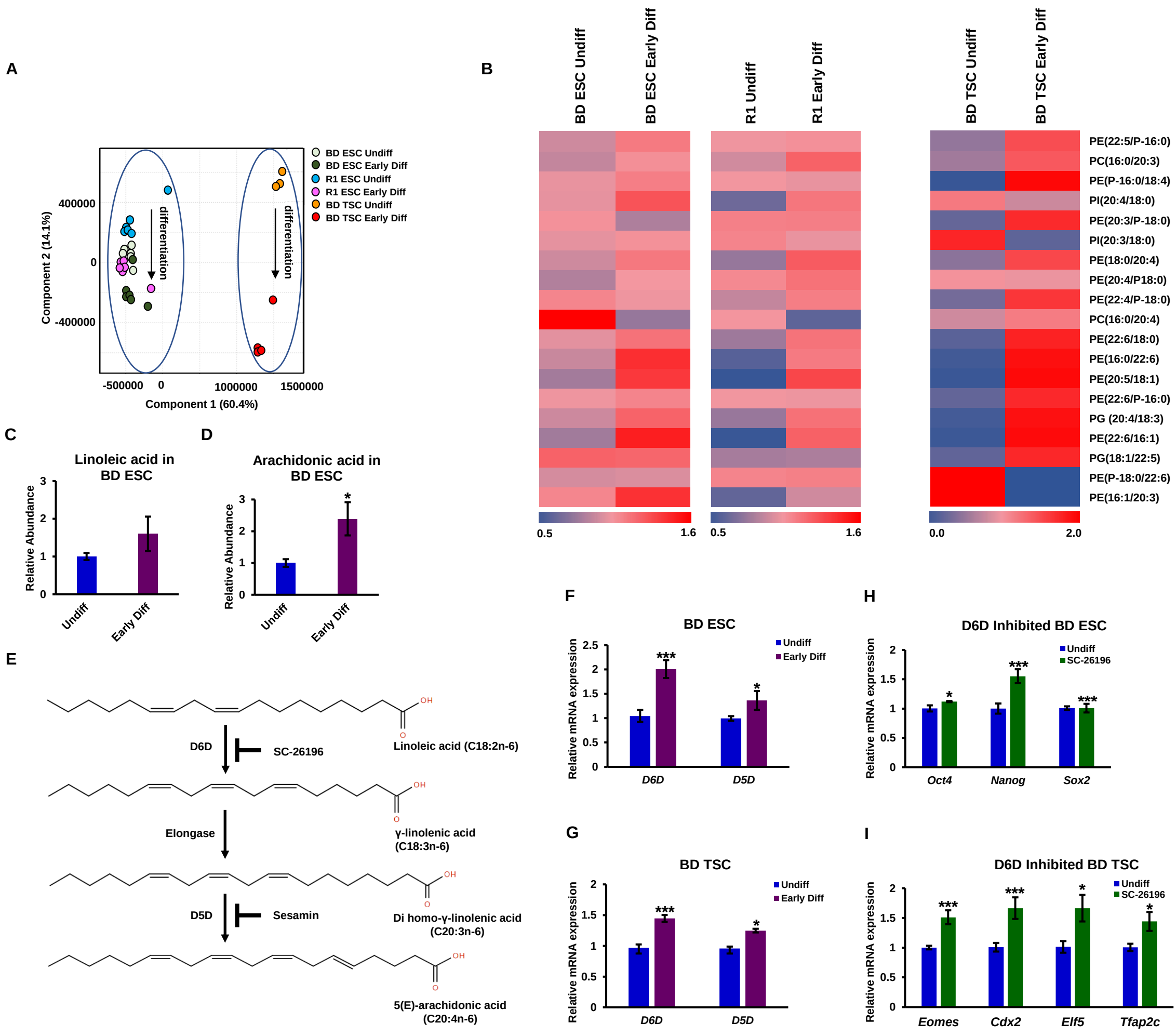
A
BD ESC Undiff
BD ESC Early Diff
R1 ESC Undiff
R1 ESC Early Diff
BD TSC Undiff
BD TSC Early Diff
differentiation
differentiation
Component 2 (14.1%)
Component 1 (60.4%)
400000
0
-400000
-500000
0
1000000
1500000
B
BD ESC Undiff
BD ESC Early Diff
R1 Undiff
R1 Early Diff
BD TSC Undiff
BD TSC Early Diff
PE(22:5/P-16:0)
PC(16:0/20:3)
PE(P-16:0/18:4)
PI(20:4/18:0)
PE(20:3/P-18:0)
PI(20:3/18:0)
PE(18:0/20:4)
PE(20:4/P18:0)
PE(22:4/P-18:0)
PC(16:0/20:4)
PE(22:6/18:0)
PE(16:0/22:6)
PE(20:5/18:1)
PE(22:6/P-16:0)
PG (20:4/18:3)
PE(22:6/16:1)
PG(18:1/22:5)
PE(P-18:0/22:6)
PE(16:1/20:3)
0.5
1.6
0.5
1.6
0.0
2.0
C
Linoleic acid in BD ESC
Relative Abundance
Undiff
Early Diff
D
Arachidonic acid in BD ESC
Relative Abundance
Undiff
Early Diff
E
D6D
SC-26196
Linoleic acid (C18:2n-6)
Elongase
γ-linolenic acid (C18:3n-6)
D5D
Sesamin
Di homo-γ-linolenic acid (C20:3n-6)
5(E)-arachidonic acid (C20:4n-6)
F
BD ESC
Undiff
Early Diff
Relative mRNA expression
D6D
D5D
G
BD TSC
Undiff
Early Diff
Relative mRNA expression
D6D
D5D
H
D6D Inhibited BD ESC
Undiff
SC-26196
Relative mRNA expression
Oct4
Nanog
Sox2
I
D6D Inhibited BD TSC
Undiff
SC-26196
Relative mRNA expression
Eomes
Cdx2
Elf5
Tfap2c

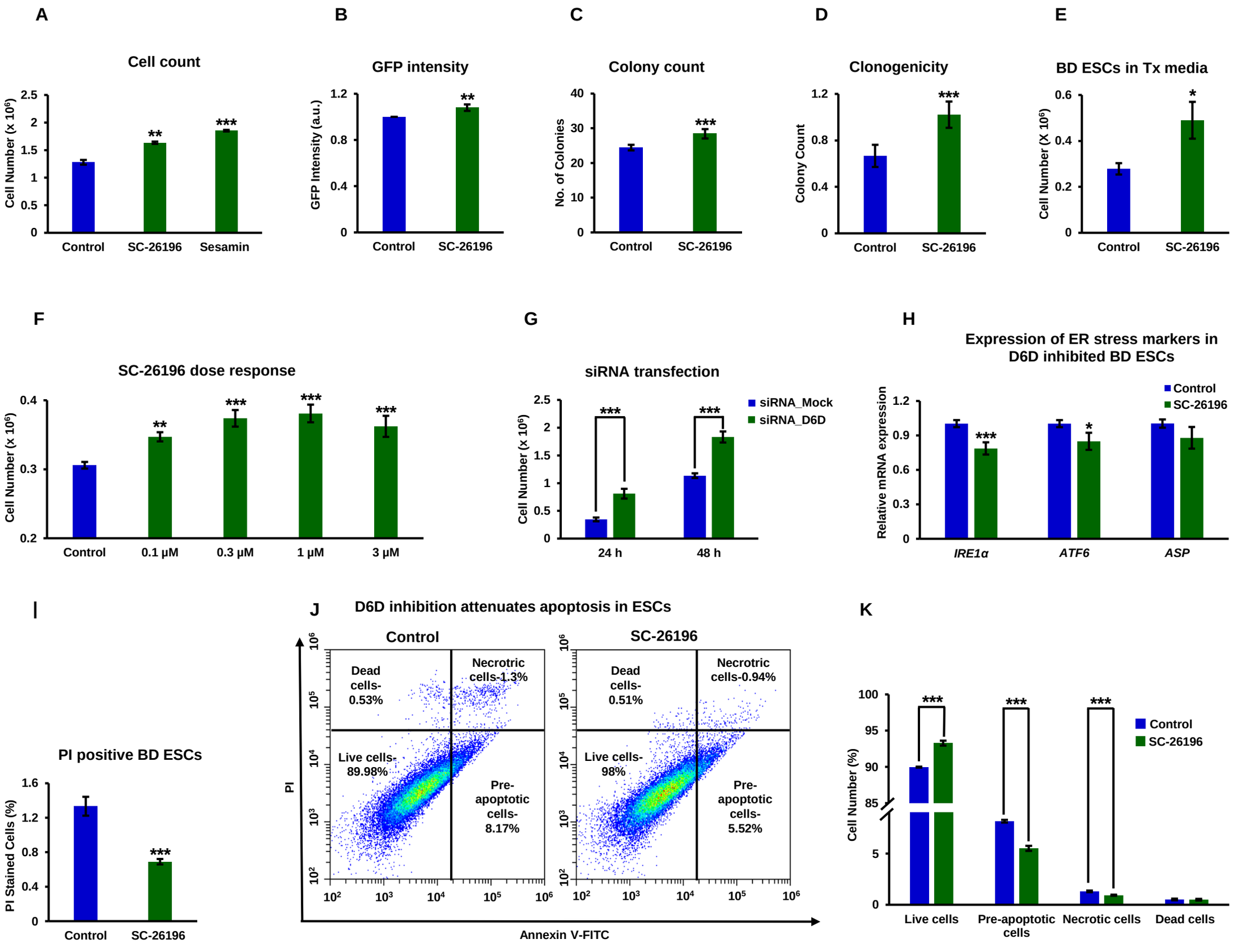
A
Cell count
Cell Number (x 10⁶)
Control
SC-26196
Sesamin
B
GFP intensity
GFP Intensity (a.u.)
C
Colony count
No. of Colonies
D
Clonogenicity
Colony Count
E
BD ESCs in Tx media
Cell Number (X 10⁶)
F
SC-26196 dose response
0.1 µM
0.3 µM
1 µM
3 µM
G
siRNA transfection
siRNA_Mock
siRNA_D6D
24 h
48 h
H
Expression of ER stress markers in D6D inhibited BD ESCs
Relative mRNA expression
IRE1α
ATF6
ASP
I
PI positive BD ESCs
PI Stained Cells (%)
J
D6D inhibition attenuates apoptosis in ESCs
Dead cells- 0.53%
Necrotric cells-1.3%
Live cells- 89.98%
Pre-apoptotic cells- 8.17%
Dead cells- 0.51%
Necrotric cells-0.94%
Live cells- 98%
Pre-apoptotic cells- 5.52%
PI
Annexin V-FITC
K
Cell Number (%)
Live cells
Pre-apoptotic cells
Necrotic cells
Dead cells

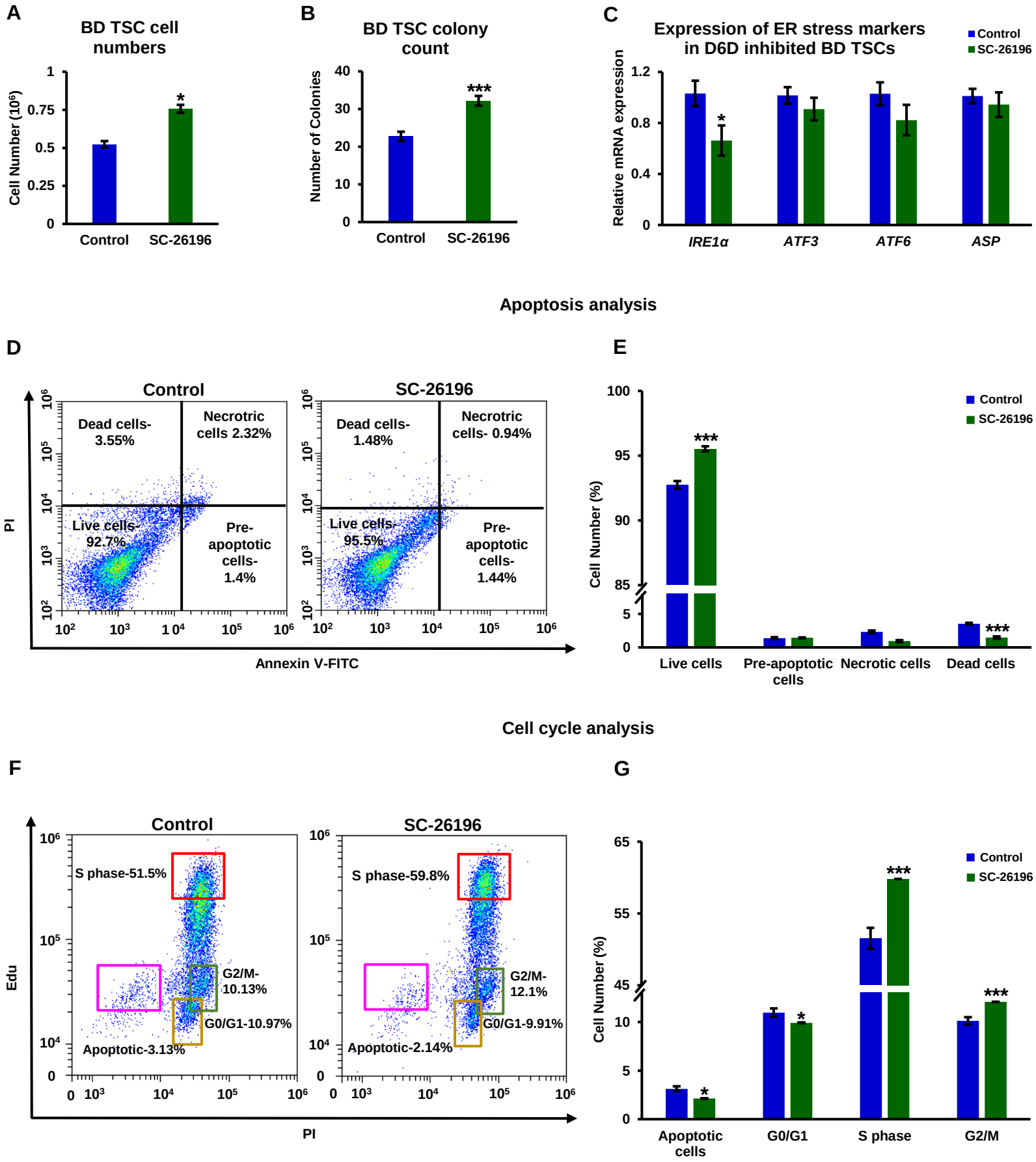
A
BD TSC cell numbers
Cell Number (10⁶)
1
0.75
0.5
0.25
0
*
Control
SC-26196
B
BD TSC colony count
Number of Colonies
40
30
20
10
0
***
Control
SC-26196
C
Expression of ER stress markers in D6D inhibited BD TSCs
Control
SC-26196
Relative mRNA expression
1.2
0.8
0.4
0
*
IRE1α
ATF3
ATF6
ASP
Apoptosis analysis
D
Control
Dead cells- 3.55%
Necrotric cells 2.32%
Live cells- 92.7%
Pre-apoptotic cells- 1.4%
SC-26196
Dead cells- 1.48%
Necrotric cells- 0.94%
Live cells- 95.5%
Pre-apoptotic cells- 1.44%
PI
Annexin V-FITC
E
Control
SC-26196
Cell Number (%)
100
95
90
85
5
0
***
***
Live cells
Pre-apoptotic cells
Necrotic cells
Dead cells
Cell cycle analysis
F
Control
S phase-51.5%
G2/M- 10.13%
G0/G1-10.97%
Apoptotic-3.13%
SC-26196
S phase-59.8%
G2/M- 12.1%
G0/G1-9.91%
Apoptotic-2.14%
Edu
PI
G
Control
SC-26196
Cell Number (%)
65
55
45
10
5
0
*
*
***
***
Apoptotic cells
G0/G1
S phase
G2/M

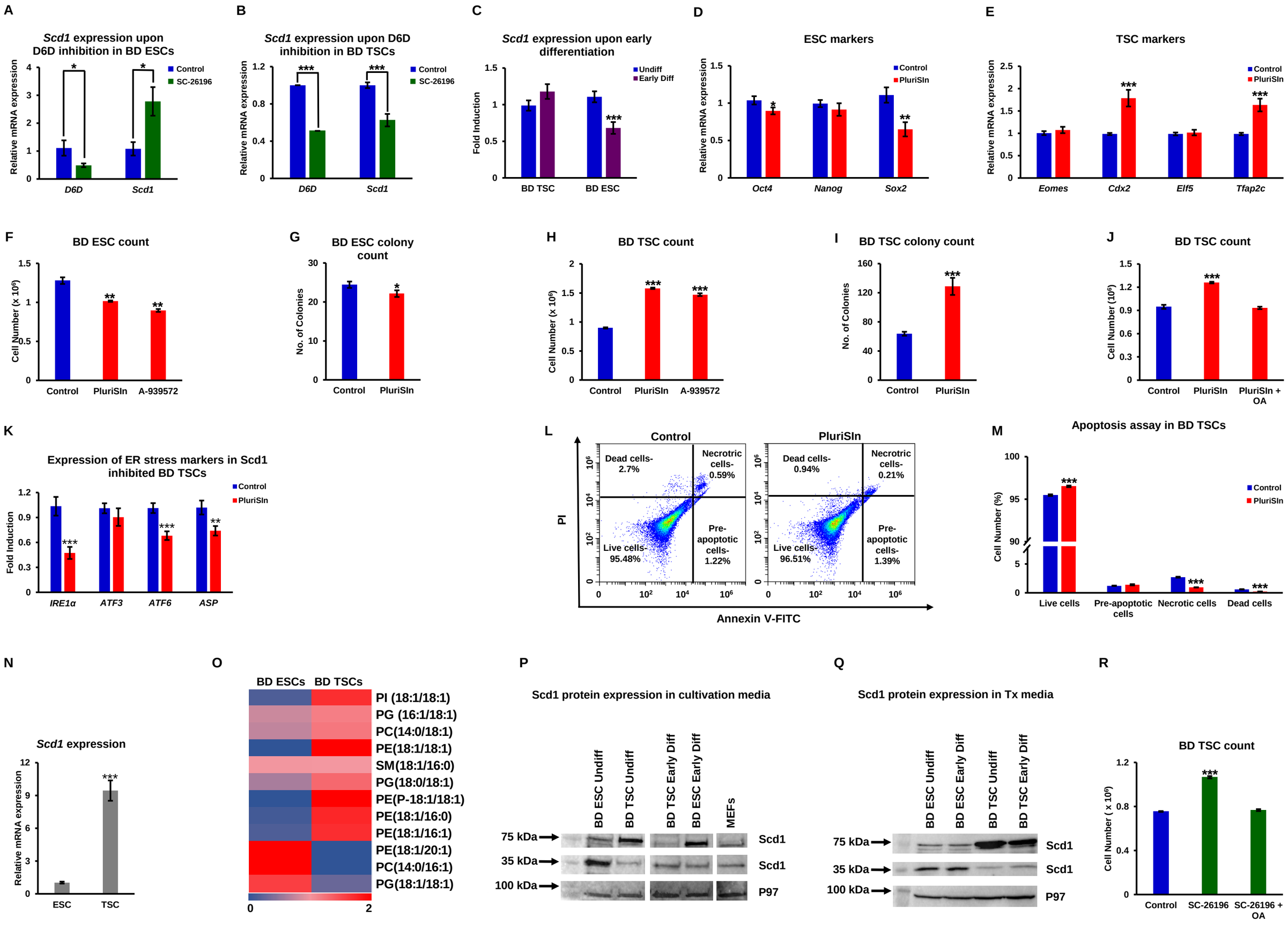
A
Scd1 expression upon D6D inhibition in BD ESCs
Relative mRNA expression
Control
SC-26196
D6D
Scd1
B
Scd1 expression upon D6D inhibition in BD TSCs
Relative mRNA expression
Control
SC-26196
D6D
Scd1
C
Scd1 expression upon early differentiation
Fold Induction
Undiff
Early Diff
BD TSC
BD ESC
D
ESC markers
Relative mRNA expression
Control
PluriSIn
Oct4
Nanog
Sox2
E
TSC markers
Relative mRNA expression
Control
PluriSIn
Eomes
Cdx2
Elf5
Tfap2c
F
BD ESC count
Cell Number (x 10⁶)
Control
PluriSIn
A-939572
G
BD ESC colony count
No. of Colonies
Control
PluriSIn
H
BD TSC count
Cell Number (x 10⁶)
Control
PluriSIn
A-939572
I
BD TSC colony count
No. of Colonies
Control
PluriSIn
J
BD TSC count
Cell Number (10⁶)
Control
PluriSIn
PluriSIn + OA
K
Expression of ER stress markers in Scd1 inhibited BD TSCs
Fold Induction
Control
PluriSIn
IRE1α
ATF3
ATF6
ASP
L
Control
PluriSIn
Dead cells- 2.7%
Necrotic cells- 0.59%
Pre-apoptotic cells- 1.22%
Live cells- 95.48%
Dead cells- 0.94%
Necrotic cells- 0.21%
Pre-apoptotic cells- 1.39%
Live cells- 96.51%
PI
Annexin V-FITC
M
Apoptosis assay in BD TSCs
Cell Number (%)
Control
PluriSIn
Live cells
Pre-apoptotic cells
Necrotic cells
Dead cells
N
Scd1 expression
Relative mRNA expression
ESC
TSC
O
BD ESCs
BD TSCs
PI (18:1/18:1)
PG (16:1/18:1)
PC(14:0/18:1)
PE(18:1/18:1)
SM(18:1/16:0)
PG(18:0/18:1)
PE(P-18:1/18:1)
PE(18:1/16:0)
PE(18:1/16:1)
PE(18:1/20:1)
PC(14:0/16:1)
PG(18:1/18:1)
P
Scd1 protein expression in cultivation media
BD ESC Undiff
BD TSC Undiff
BD TSC Early Diff
BD ESC Early Diff
MEFs
75 kDa
35 kDa
100 kDa
Scd1
Scd1
P97
Q
Scd1 protein expression in Tx media
BD ESC Undiff
BD ESC Early Diff
BD TSC Undiff
BD TSC Early Diff
75 kDa
35 kDa
100 kDa
Scd1
Scd1
P97
R
BD TSC count
Cell Number (x 10⁶)
Control
SC-26196
SC-26196 + OA